Cysteinyl leukotriene 2 receptor promotes endothelial permeability, tumor angiogenesis, and metastasis

Ernest Duah[a,1], Lakshminarayan Reddy Teegala[a,1], Vinay Kondeti[a], Ravi K. Adapala[b], Venkateshwar G. Keshamouni[c], Yoshihide Kanaoka[d,e], K. Frank Austen[d,e,2], Charles K. Thodeti[b], and Sailaja Paruchuri[a,2]

[a]Department of Chemistry, University of Akron, Akron, OH 44325; [b]Department of Integrative Medical Sciences, Northeast Ohio Medical University, Rootstown, OH 44272; [c]Division of Pulmonary and Critical Care Medicine, Department of Internal Medicine, University of Michigan, Ann Arbor, MI 48109; [d]Division of Rheumatology, Immunology, and Allergy, Brigham and Women's Hospital, Boston, MA 02115; and [e]Department of Medicine, Harvard Medical School, Boston, MA 02115

Contributed by K. Frank Austen, November 12, 2018 (sent for review October 9, 2018; reviewed by Timothy T. Hla and Roy J. Soberman)

Cysteinyl leukotrienes (cys-LTs) are proinflammatory mediators that enhance vascular permeability through distinct receptors (CysLTRs). We found that $CysLT_2R$ regulates angiogenesis in isolated mouse endothelial cells (ECs) and in Matrigel implants in WT mice and enhances EC contraction and permeability via the Rho-dependent myosin light chain 2 and vascular endothelial (VE)-cadherin axis. Since solid tumors utilize aberrant angiogenesis for their growth and metastasis and their vessels exhibit vascular hyperpermeability, we hypothesized that $CysLT_2R$, via its actions on the endothelium, might regulate tumor growth. Both tumor growth and metastases of adoptively transferred syngeneic Lewis lung carcinoma (LLC) cells are significantly reduced in $CysLT_2R$-null mice (*Cysltr2*$^{-/-}$) compared with WT and $CysLT_1R$-null mice (*Cysltr1*$^{-/-}$). In WT recipients of LLC cells, $CysLT_2R$ expression is significantly increased in the tumor vasculature, compared with $CysLT_1R$. Further, the tumor vasculature in *Cysltr2*$^{-/-}$ recipients exhibited significantly improved integrity, as revealed by increased pericyte coverage and decreased leakage of i.v.-administered Texas Red-conjugated dextran. Administration of a selective $CysLT_2R$ antagonist significantly reduced LLC tumor volume, vessel density, dextran leakage, and metastases in WT mice, highlighting $CysLT_2R$ as a VEGF-independent regulator of the vasculature promoting risk of metastasis. Thus, both genetic and pharmacological findings establish $CysLT_2R$ as a gateway for angiogenesis and EC dysregulation in vitro and ex vivo and in an in vivo model with a mouse tumor. Our data suggest $CysLT_2R$ as a possible target for intervention.

cysteinyl leukotriene receptors | angiogenesis | endothelial cells | metastasis | tumor growth

Cysteinyl leukotrienes (cys-LTs) are proinflammatory mediators generated from arachidonic acid by the action of 5-lipoxygenase (5-LO) in the presence of the 5-LO activating protein (FLAP) to provide LTA_4 for conjugation to reduced glutathione by LTC_4 synthase (LTC_4S) (1). LTC_4, the initial biosynthetic ligand, is exported, and extracellular cleavage of the peptide adduct removes glutamic acid and then glycine to sequentially provide LTD_4 and LTE_4. Although cys-LTs are mainly secreted by infiltrating LTC_4S-containing inflammatory cells (2), endothelial cells (ECs) can take up LTA_4 released by leukocytes and generate cys-LTs using microsomal GST-2 and gamma-glutamyl transpeptidases (3). ECs are activated by proinflammatory mediators generated during inflammation, and the progression of endothelial inflammatory responses is linked to angiogenesis (4, 5). Injection of each of the three cys-LTs has been shown to enhance dermal vascular permeability in mice and humans (6–8). Individual receptors have also been demonstrated to mediate particular responses in mice, such as allergic pulmonary inflammation via $CysLT_1R$ receptor ($CysLT_1R$) on dendritic cells (9), skin fibrosis via $CysLT_2R$ in a model of atopic dermatitis (10), and mucus secretion by $CysLT_3R$ on goblet cells (11, 12). $CysLT_2R$ with a Leu129Gln mutation has been identified as a uveal melanoma oncogene, acting via $G\alpha_q$ signaling (13). Using specific pharmacological antagonists and null strains for the classical receptors $CysLT_1R$ and $CysLT_2R$, we find a striking role for $CysLT_2R$ in angiogenesis and EC function in normal tissues and in a Lewis lung carcinoma (LLC) tumor and its metastasis. Indeed, deletion or inhibition of $CysLT_2R$ stabilizes tumor vasculature integrity and reduces metastases.

Results

Ligand-Induced $CysLT_2R$-Dependent Angiogenesis. To determine if cys-LTs influence angiogenesis, we first assessed the ability of different doses of LTD_4 to impact tube formation of mouse dermal ECs (MDECs) on Matrigel in an in vitro angiogenesis assay. Compared with the control, the number of tubes formed in LTD_4-treated cells was significantly higher (Fig. 1 *A* and *B*). LTC_4 and LTD_4 were equipotent in forming tubes in the Matrigel in vitro assay (*SI Appendix*, Fig. S1*C*). Next, the ex vivo aortic ring assay revealed that LTD_4 induced significant angiogenesis, as shown by numerous vessel sprouts from the aortic rings in comparison to the control aortic rings (Fig. 1 *C* and *D*). The effect of LTD_4 on angiogenesis in vivo was examined by implanting Matrigel plugs supplemented with suboptimal concentrations of basic fibroblast growth factor (bFGF; 200 ng/mL) alone (control) or in the presence of LTD_4 (500 nM) under the flanks of WT mice (14). LTD_4 treatment significantly enhanced blood vessel formation compared with the control, as evidenced by CD31 staining of ECs in sections from the harvested Matrigel plugs (Fig. 1 *E* and *F*). LTD_4-induced angiogenesis in plugs was significantly attenuated in *Cysltr2*$^{-/-}$ mice compared with WT and *Cysltr1*$^{-/-}$ mice (Fig. 1

Significance

Cysteinyl leukotrienes (cys-LTs) are proinflammatory mediators and regulate endothelial cell contraction, permeability, and angiogenesis via a cys-LT receptor, $CysLT_2R$. In response to the challenges of finding therapies that can combat tumor angiogenesis and metastases, we explored the advantage of targeting this receptor. We show that $CysLT_2R$ mediates tumor angiogenesis and contributes to metastasis in vivo independent of VEGF by enhancing leakiness and permeability of blood vessels. We propose that a $CysLT_2R$ antagonist, $BayCysLT_2$, can normalize vessels, reducing tumor growth and metastasis.

Author contributions: C.K.T. and S.P. designed research; E.D., L.R.T., V.K., and R.K.A. performed research; Y.K. and K.F.A. contributed new reagents/analytic tools; E.D., L.R.T., V.K., and R.K.A. analyzed data; and E.D., L.R.T., V.K., R.K.A., V.G.K., Y.K., K.F.A., C.K.T., and S.P. wrote the paper.

Reviewers: T.T.H., Boston Children's Hospital and Harvard Medical School; and R.J.S., Massachusetts General Hospital.

The authors declare no conflict of interest.

[1]E.D. and L.R.T. contributed equally to this work.

[2]To whom correspondence may be addressed. Email: fausten@research.bwh.harvard.edu or sp97@uakron.edu.

This article contains supporting information online at www.pnas.org/lookup/suppl/doi:10.1073/pnas.1817325115/-/DCSupplemental.

Published online December 17, 2018.

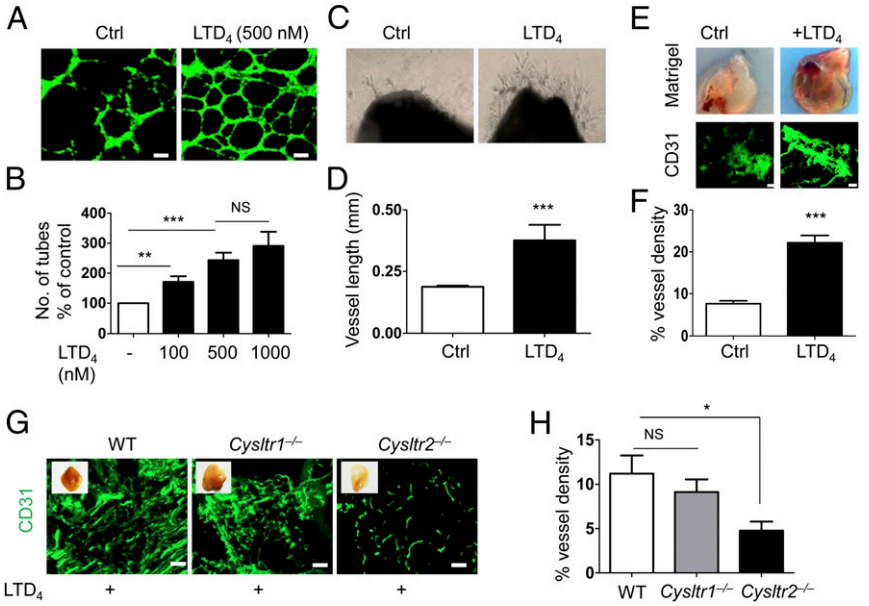

Fig. 1. LTD_4 induces angiogenesis through $CysLT_2R$. (*A* and *B*) MDECs were plated on growth factor-reduced Matrigel and treated with or without LTD_4 (100, 500, and 1,000 nM) for 12–16 h. Cells were stained with calcein AM and fixed. (*A*) Representative images of tube formation with and without LTD_4 (500 nM) treatment. Ctrl, control. (Scale bars: 200 μm.) (*B*) Quantification of tube formation. Tubes from at least 10 representative images of each replicate were counted manually and presented as the average percentage from three separate experiments. (*C*) Representative photographs of aortic rings from WT mice placed in growth factor-reduced Matrigel and then treated with or without LTD_4 for 7 d. (*D*) Quantification of sprout length (n = 6–8). (*E*–*H*) Growth factor-reduced Matrigel supplemented with bFGF (200 ng/mL) alone (Ctrl) or in the presence of LTD_4 (500 nM) was injected into both flanks of indicated mouse groups for 21 d. (*E*, *Upper*) Representative photographs of Matrigel plugs. (*E*, *Lower*) Matrigel sections immunostained for CD31. (Scale bars: 100 μm.) (*F*) Quantification of CD31 fluorescence (n = 10 per group) from *E*. (*G*) Representative CD31-stained Matrigel plug sections from the indicated mouse groups. (Scale bars: 100 μm.) (*H*) Quantification of CD31 staining from *G* (n = 8–12 per group). Data are shown as mean ± SEM. $^*P < 0.05$; $^{**}P < 0.01$; $^{***}P < 0.001$; NS (nonsignificant) as determined by the Mann–Whitney *U* test (*B*, *D*, and *F*) and one-way ANOVA with a Tukey post hoc test (*H*).

G and *H*). In addition, mouse lung ECs (MLECs) isolated from *Cysltr2*$^{-/-}$ mice exhibited diminished potential to form tubes in vitro compared with ECs isolated from WT and *Cysltr1*$^{-/-}$ mice using the in vitro angiogenesis assay (*SI Appendix*, Fig. S1 *A* and *B*). The in vitro, ex vivo, and in vivo assays of angiogenesis indicated $CysLT_2R$ as the preferred receptor to LTD_4 compared with $CysLT_1R$.

$CysLT_2R$ Signaling Enhances Endothelial Contraction and Permeability. To gain functional insights on $CysLT_2R$ signaling in angiogenesis and vascular integrity, we measured EC contraction and permeability. Consistent with our previous findings with human umbilical vein ECs (HUVECs) (15), LTD_4 stimulation induced contraction, with formation of large gaps in the monolayer of MLECs from WT and *Cysltr1*$^{-/-}$ mice. In contrast, LTD_4 failed to increase contraction and gap formation in MLECs isolated from *Cysltr2*$^{-/-}$ mice (Fig. 2 *A* and *B*). We next observed that LTD_4 induced a twofold increase in the permeability of WT MLECs on gelatin-coated transwell inserts assayed by flux of added Texas Red-conjugated dextran. Basal *Cysltr1*$^{-/-}$ MLEC permeability was higher compared with that of basal WT or *Cysltr2*$^{-/-}$ ECs, and was even further augmented with LTD_4. In contrast, LTD_4 did not significantly increase permeability of ECs from *Cysltr2*$^{-/-}$ mice (Fig. 2*C*). To understand the molecular mechanism behind $CysLT_2R$-induced EC contraction and permeability of WT ECs, we focused on the Rho axis as the Rho kinase (ROCK) inhibitor (Y27632) has been shown to abrogate $CysLT_2R$-induced contraction in HUVECs (15). We found that the ROCK inhibitor blocked permeability in WT MLECs (Fig. 2*C*). Further, LTD_4 stimulation increased ROCK activity (Fig. 2*D*) as well as phosphorylation of myosin light chain 2 (MLC-2) at ser19 in human dermal microvascular ECs (HDMECs) (Fig. 2*E*), which was attenuated in the presence of $BayCysLT_2$, a $CysLT_2R$ antagonist (Fig. 2*E*). We observed time-dependent phosphorylation of MLC-2 with LTD_4 in WT and *Cysltr1*$^{-/-}$ MLECs, but not in *Cysltr2*$^{-/-}$ MLECs (Fig. 2*F*), indicating an important similarity of $CysLT_2R$ function in both human and mouse ECs. Next, we asked if $CysLT_2R$ destabilized EC/EC junctions and promoted permeability by disrupting vascular endothelial (VE)-cadherin (Cadh5) expression (16). LTD_4 induced a time-dependent disruption of VE-cadherin expression at the EC/EC junctions in HDMECs (Fig. 2*G*) and in WT and *Cysltr1*$^{-/-}$ MLECs (Fig. 2*H*), but did not cause any change in *Cysltr2*$^{-/-}$ MLECs. Since VEGF is the major driver for angiogenesis, we stimulated ECs (HDMECs and HUVECs) with LTD_4 or VEGF for 15 min and then measured the phosphorylation of VEGF and downstream effectors of the VEGF pathway. We detected phosphorylation of VEGF receptor (VEGFR), NF-κB, PLC-γ, Erk, and P38 MAPK upon stimulation with VEGF, but not with LTD_4 (*SI Appendix*, Fig. S2 *A*–*C*). In addition, the VEGF-induced phosphorylation of PLC-γ and Erk was unaffected by treatment with either the $CysLT_1R$ antagonist MK571 or the $CysLT_2R$ antagonist $BayCysLT_2$ (*SI Appendix*, Fig. S2 *D*–*F*). Similarly, the VEGFR inhibitor sunitinib attenuated VEGF-induced Erk phosphorylation (*SI Appendix*, Fig. S2*G*) but failed to inhibit LTD_4-induced MLEC contraction (*SI Appendix*, Fig. S2*H*). These data indicate that LTD_4 signaling does not transactivate VEGFR in ECs of human origin.

Genetic Deletion of $CysLT_2R$ Diminishes Angiogenesis and Growth of Transplanted LLC Cells. To determine if $CysLT_2R$ also mediates pathological angiogenesis, we implanted syngeneic LLC cells by s.c. injection in the flanks of WT, *Cysltr1*$^{-/-}$, and *Cysltr2*$^{-/-}$ mice, and measured tumor growth and angiogenesis over 3 wk (Fig. 3*A*). Tumor volume was robust but significantly less at days 18 and 21 in *Cysltr2*$^{-/-}$ mice compared with WT and *Cysltr1*$^{-/-}$ mice (Fig. 3 *B* and *C*). Notably, there was an associated reduction in tumor angiogenesis in *Cysltr2*$^{-/-}$ mice in comparison to WT and *Cysltr1*$^{-/-}$ mice, as evidenced by CD31 staining (Fig. 3 *D* and *E*). There was no apparent difference in recruitment of leukocytes to the tumor,

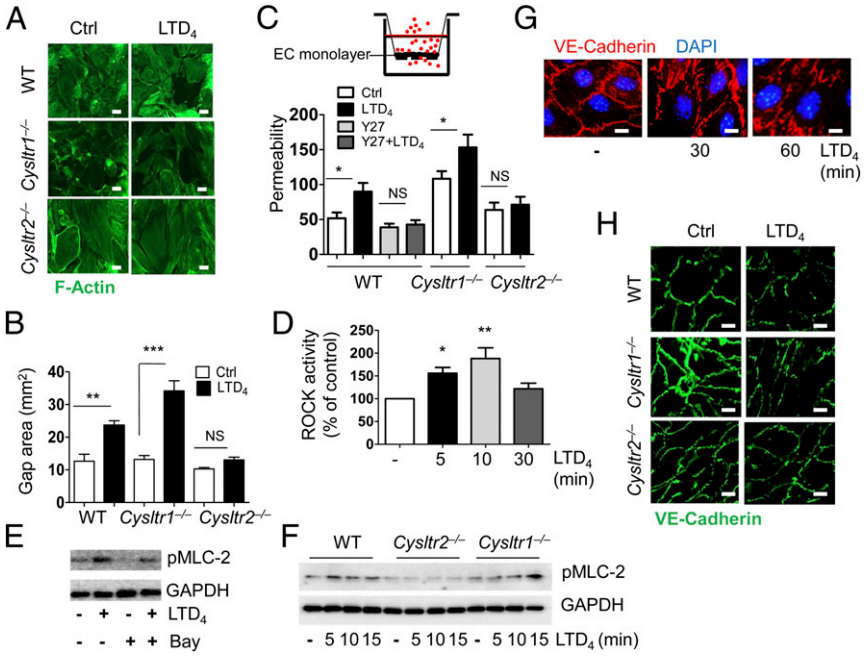

Fig. 2. LTD_4 regulates EC contraction and permeability through the $CysLT_2R$/ROCK/MLC-2/VE-cadherin axis. (*A*) Representative fluorescence micrographs of ECs from indicated mouse groups stained with phalloidin (F-actin, green), showing an increase in gap formation after treatment with LTD_4 (500 nM; 1 h). Ctrl, control. (Scale bars: 20 μm.) (*B*) Quantification of gap formation by LTD_4 (500 nM). (*C*) Permeability of MLECs from the indicated mouse groups. ECs were cultured on gelatin-coated transwell inserts; incubated with Y27 (10 μM; Y27632) for 30 min; and stimulated with or without LTD_4 (500 nM) for 1 h. Media were replaced with media containing 2 mg/mL Texas Red-conjugated dextran and incubated for an additional 1 h. Media from the bottom wells were taken, and fluorescence intensities were measured. (*D*) Time-dependent increase in ROCK activity after LTD_4 stimulation (500 nM) in ECs. Western blots show LTD_4-induced phosphorylation of MLC-2 in HDMECs (*E*) and MLECs (*F*) from the indicated mouse groups. GAPDH was used as a loading control. (*G*) Time-dependent disruption of VE-cadherin (red) junctions in HDMECs with 500 nM LTD_4 stimulation. (Scale bars: 20 μm.) (*H*) LTD_4-induced disruption of VE-cadherin (green) junctions in MLECs from the indicated mouse groups. (Scale bars: 20 μm.) Data are shown as mean ± SEM of at least three different experiments, $*P < 0.05$; $**P < 0.01$; $***P < 0.001$; NS (nonsignificant) determined by one-way ANOVA with Tukey multiple comparison test.

as determined by CD45 staining of WT, *Cysltr1*$^{-/-}$, and *Cysltr2*$^{-/-}$ mice (Fig. 3 *D* and *F*). Of note was the finding that $CysLT_2R$ expression is higher than $CysLT_1R$ expression in the tumor vasculature of WT mice, as revealed by the double-staining of CD31 and CysLTRs (Fig. 3 *G* and *H*).

$CysLT_2R$ Deficiency Stabilizes Tumor Vascular Integrity and Reduces Lung Metastasis of Transplanted LLC Cells. Analysis of LLC tumor metastasis to lungs revealed that *Cysltr2*$^{-/-}$ mice had significantly fewer metastatic foci (mets) compared with WT and *Cysltr1*$^{-/-}$ mice (Fig. 4 *A* and *B*). Further, mets in *Cysltr2*$^{-/-}$ mice were notably smaller compared with WT and *Cysltr1*$^{-/-}$ mice, as determined by the total area of mets occupied per lung (Fig. 4*C*). We next investigated the integrity of tumor vessels by analyzing pericyte coverage. Costaining of the tumor vessels with both an EC marker (CD31) and a pericyte marker (NG2) revealed that tumors from both WT and *Cysltr1*$^{-/-}$ mice exhibited minimal pericyte coverage, indicative of immature and malformed vessels, as typically seen in tumor vasculature (17, 18). In contrast, although the vessel density in tumors of *Cysltr2*$^{-/-}$ mice is low, we observed high pericyte coverage of the tumor vessels, which is indicative of integrity (Fig. 4 *D*–*F*; colocalization of CD31 and NG2). There was ∼90% pericyte coverage in the tumor vasculature of *Cysltr2*$^{-/-}$ mice compared with 40% in WT mice or 25% in *Cysltr1*$^{-/-}$ mice (Fig. 4*F*). To determine the leakiness of vessels, Texas Red-conjugated dextran was injected into the tail vein of tumor-bearing WT, *Cysltr1*$^{-/-}$, and *Cysltr2*$^{-/-}$ mice 20 min before death. *Cysltr2*$^{-/-}$ mice displayed a significant reduction in dextran leakage (∼80% reduction; $P = 0.008$) compared with WT or *Cysltr1*$^{-/-}$ mice (Fig. 4 *G* and *H*). Together, these findings suggest that the reduced metastasis in the absence of $CysLT_2R$ is related to greater vessel integrity.

Comparing MLECs, we found that those from *Cysltr2*$^{-/-}$ mice expressed reduced basal transcripts for *bFGF* (EC growth factor), considered essential for angiogenesis, compared with WT and *Cysltr1*$^{-/-}$ mice. They also had augmented transcripts for platelet-derived growth factor (*PDGF*; EC growth factor), considered responsible for pericyte recruitment, compared with WT and *Cysltr*$^{-/-}$ mice (*SI Appendix*, Fig. S1 *D* and *E*).

$CysLT_2R$ Antagonist Reduces Tumor Growth and Lung Metastases. To support the genetic findings for the role of $CysLT_2R$ in tumor angiogenesis and metastasis in vivo, we assessed these parameters in normal mice in the presence or absence of the specific $CysLT_2R$ antagonist $BayCysLT_2$. We validated the specificity of $BayCysLT_2$ using CHO cells stably expressing $CysLT_1R$ (CHO-$CysLT_1R$) or $CysLT_2R$ (CHO-$CysLT_2R$) (19). In response to LTD_4, CHO-$CysLT_1R$ cells fluxed calcium (*SI Appendix*, Fig. S3*A*) and induced Erk phosphorylation (*SI Appendix*, Fig. S3*B*), which is sensitive to MK571 but not to $BayCysLT_2$. Conversely, LTD_4-induced modest calcium flux (*SI Appendix*, Fig. S3*A*) and Erk phosphorylation (*SI Appendix*, Fig. S3*B*) in CHO-$CysLT_2R$ cells is sensitive to $BayCysLT_2$ but not to MK571. We also established that $BayCysLT_2$ had no effect on proliferation of LLC cells in vitro and that the LLC cells expressed both receptors (*SI Appendix*, Fig. S4).

WT mice were injected s.c. with LLC cells, and when the tumor size reached 100 mm^3, they were treated with saline or $BayCysLT_2$ (3 mg/kg of body weight) (20) by i.p. injection on the seventh day, with repeated doses on alternate days up to the 18th day. $BayCysLT_2$-treated mice showed a statistically significant reduction in tumor volume in comparison to saline treatments (Fig. 5 *A*–*C*). $BayCysLT_2$ reduced lung metastasis significantly ($P = 0.03$) compared

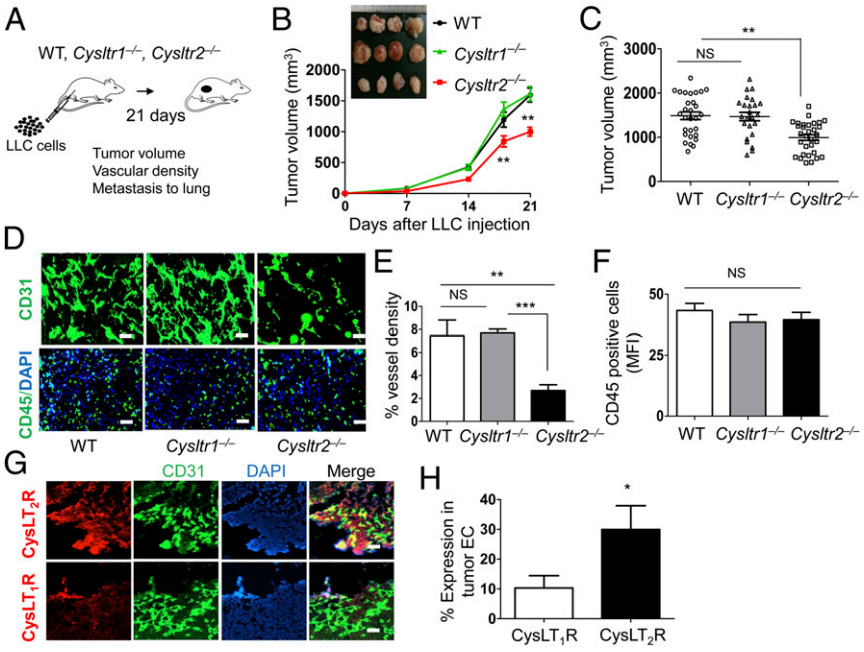

Fig. 3. Genetic deletion of $CysLT_2R$ inhibits tumor angiogenesis and growth. (*A*) Cartoon showing the outline of tumor experiment. LLC cells (2×10^6 in 100 μL of PBS) were injected s.c. into both flanks of the indicated mouse groups. On day 21, mice were euthanized, tumor volume was measured, and primary tumors were harvested for histological studies. (*B*) Time-dependent change in tumor growth (volume) in the indicated mouse groups. (*Inset*) Photographs of primary tumors. (*C*) Tumor volumes of indicated mouse groups at day 21. (*D*) Representative fluorescence images showing vessel density (CD31, green) and $CD45^+$ cells (CD45, green; DAPI, blue) in tumor sections from indicated mouse groups. (Scale bars: 100 μm.) (*E*) Quantification of vessel density from *D*. (*F*) Quantification of $CD45^+$ cells from *D*. (*G*) Immunofluorescence images of tumor sections from WT mice showing the expression of $CysLT_1R$ and $CysLT_2R$ (red) in the tumor vessels (CD31, green). Nuclei were stained with DAPI (blue). ($n = 5$ per group). (Scale bars: 100 μm.) (*H*) Quantification of $CysLT_1R$ and $CysLT_2R$ expression in tumor vasculature. Data are shown as mean ± SEM. $^*P < 0.05$; $^{**}P < 0.01$; $^{***}P < 0.001$; NS (nonsignificant) as determined by one-way ANOVA with a Tukey post hoc test or the Mann–Whitney *U* test (in *H*).

with saline treatment (Fig. 5 *D*–*F*). Further, $BayCysLT_2$-treated tumors exhibited significantly reduced vessel density, increased pericyte coverage, and reduced dextran leakage (Fig. 5 *G*–*J*). We did not observe any difference in the $CD45^+$ immune cells between saline- and $BayCysLT_2$-treated tumors (Fig. 5*K*).

Discussion

Our study demonstrates that $CysLT_2R$ can promote angiogenesis and EC contraction with permeability not only in vitro and ex vivo with a specific agonist but also spontaneously in vivo in a tumor model. Following flank injection of syngeneic LLC cells,

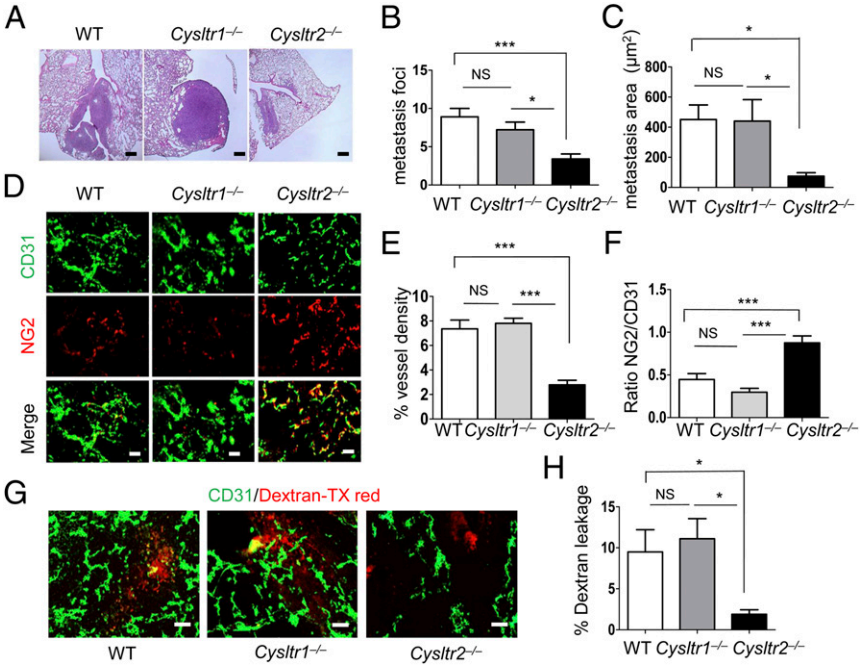

Fig. 4. Absence of $CysLT_2R$ normalizes tumor vasculature and inhibits tumor metastasis. LLC cells (2×10^6 in 100 μL of PBS) were injected s.c. in both flanks of the indicated mouse groups. On day 21, mice were euthanized and lungs were harvested for histological studies. (*A*) H&E staining of the lungs showing metastasis. (Scale bar: 200 μm.) Metastasis foci (*B*) and quantification of the metastasis area (*C*) are shown. (*D*) Representative immunofluorescence images of tumors of the indicated mouse groups stained with an endothelial marker (CD31, green) and pericyte marker (NG2, red), and merged ($n = 10$–15 per group). (Scale bars: 100 μm.) Quantification of tumor vessel density (*E*; CD31, green) and pericyte coverage (*F*; NG2, pericyte in red/CD31, EC in green) from the indicated mouse groups. (*G*) Tumor sections from the indicated mouse groups injected with Texas (TX) Red-conjugated dextran and stained with CD31, showing the leakiness of the vessels ($n = 10$–12 per group). (Scale bars: 100 μm.) (*H*) Quantification of Texas Red-conjugated dextran leakage into the tumor tissue. Data are shown as mean ± SEM. $^*P < 0.05$; $^{***}P < 0.001$; NS (nonsignificant) determined by one-way ANOVA with a Tukey post hoc test.

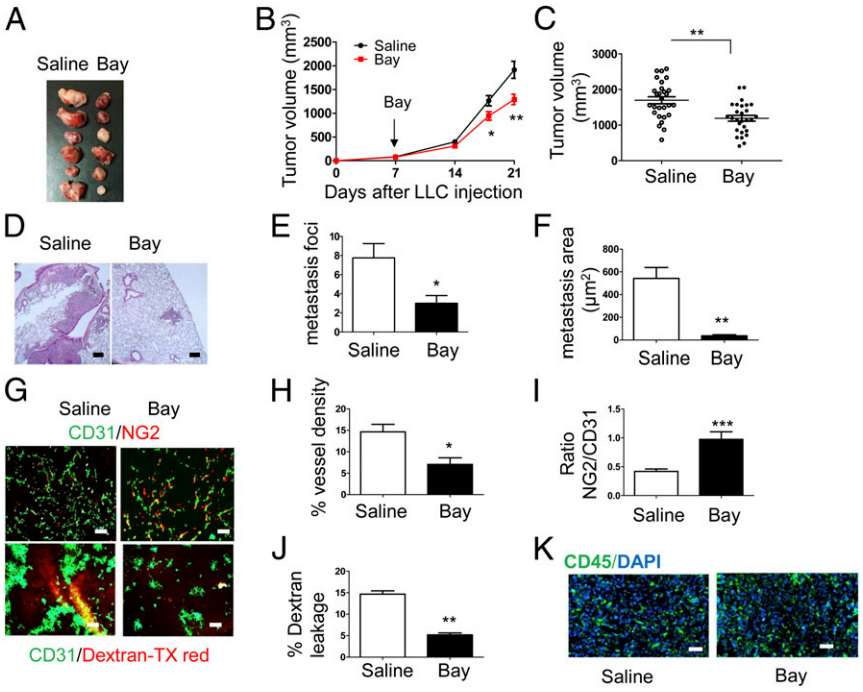

Fig. 5. Effect of pharmacological targeting of $CysLT_2R$ with $BayCysLT_2$. (*A–K*) LLC cells (2×10^6 in 100 μL of PBS) were injected s.c. into both flanks of 6- to 8-wk-old WT mice. When tumors were palpable on the seventh day, mice were randomized into two groups. One group was injected (i.p.) with 3 mg/kg of Bay ($n = 10$; $BayCysLT_2$), and the other group was injected with saline ($n = 10$) as a vehicle control every other day (five doses). On day 21 after tumor transplantation, mice were injected with Texas Red-conjugated dextran 20 min before euthanasia. Treatment with $BayCysLT_2$ inhibits tumor volume (*A–C*), metastasis to the lung (*D* and *E*), and metastatic area (*F*). (Scale bars: 200 μm.) (*G*) Immunofluorescence images of tumor sections showing pericyte coverage (CD31/NG2 staining, *Upper*) and leakage of Texas (TX) Red-conjugated dextran (*Lower*). (Scale bars: 100 μm.) Quantification of vessel density (*H*), pericyte coverage (*I*), and leakage of TX Red-conjugated dextran (*J*) are shown. (*K*) Immunofluorescence images of tumor sections showing $CD45^+$ cells infiltrating the tumor (CD31, green; DAPI, blue). (Scale bars: 100 μm.) Data are shown as mean ± SEM. $^*P < 0.05$; $^{**}P < 0.01$; $^{***}P < 0.001$ determined by the Mann–Whitney *U* test.

both the local tumor and the lung metastasis in WT and $CysLT_1R$-deficient mice show marked angiogenesis and vascular dysplasia. In contrast, the $CysLT_2R$-deficient mice have significantly less tumor mass, and especially a smaller number and size of metastases, in association with much reduced angiogenesis and vascular dysplasia. Most importantly, growth of the tumor mass and of the number and size of metastases in WT mice could be attenuated while in progress by introduction of a $CysLT_2R$ antagonist. The compelling genetic and pharmacological findings for $CysLT_2R$ in angiogenesis and vascular dysplasia and their absence for $CysLT_1R$ highlight the possible therapeutic implications of our findings. Of additional interest is that the cys-LT/$CysLT_2R$ pathway for these vascular effects reflects a path independent of VEGF.

Proinflammatory cys-LTs and $CysLT_1R$ are well recognized for their role in asthma and allergic diseases. In models of vascular biology, $CysLT_2R$ is dominantly expressed in ECs (HUVECs), and it drives a proinflammatory gene expression phenotype similar to that obtained with stimulation of protease-activated receptors (21). Although $CysLT_2R$ has been implicated in vascular leakage in mouse models of pathological retinal neovascularization (22) and ischemia reperfusion (23), the functional mechanism by which cys-LTs/CysLTRs mediate these effects is not known. Vascular leakage is facilitated by endothelial permeability, which is regulated by the tensile forces within the EC monolayer and Rho family GTPases (24). Herein, we show that $CysLT_2R$ regulates EC permeability by modulating the Rho/MLC-2/VE-cadherin axis. Phosphorylation of MLC-2 triggers dissociation of β-catenin from the VE/cadherin complex, forming gaps between ECs (25), and enhances permeability. A role for cys-LTs in EC proliferation and migration has been shown in vitro or ex vivo (26–28) or in zebrafish (29). Importantly, most of these studies were conducted in macrovascular ECs (HUVECs) and not in microvascular ECs, which mainly influence angiogenesis. Using microvascular ECs (HDMECs and MLECs from *Cysltr*$^{-/-}$ strains), we unequivocally demonstrate that LTD_4 potentiates angiogenesis in vitro and in vivo via $CysLT_2R$.

Cys-LTs are mainly secreted by innate infiltrating inflammatory cells (2) and ECs (via transcellular biosynthesis) (3), and CysLTRs are expressed in both tumor (LLC) and stromal cells. Although $CysLT_2R$ was expressed in LLC cells implanted in all three strains of mice, vessel density and metastasis of tumor cells to the lung were significantly decreased in *Cysltr2*$^{-/-}$ mice compared with WT and *Cysltr1*$^{-/-}$ mice, suggesting that $CysLT_2R$ expression in stromal cells, rather than tumor cells, is essential for enhanced vascular permeability, angiogenesis, and metastasis. Further, we found similar levels of localization of $CD45^+$ leukocytes to the tumors in WT, *Cysltr1*$^{-/-}$, and *Cysltr2*$^{-/-}$ mice.

It was not evident why and how an inflammatory receptor influenced tumor metastasis. The number of vessels was fewer in LLC tumors in the *Cysltr2*$^{-/-}$ mice compared with tumors in WT or *Cysltr1*$^{-/-}$ mice. Importantly, vessel integrity was significantly disrupted in tumors in the WT or *Cysltr1*$^{-/-}$ mice compared with the *Cysltr2*$^{-/-}$ mice, as assessed by pericyte coverage or leak of labeled dextran administered systemically. Moreover, lung-derived ECs in *Cysltr2*$^{-/-}$ mice expressed enhanced PDGF, which is essential for pericyte recruitment (30), and reduced bFGF transcript, which is essential for angiogenesis (31). Our result that $CysLT_2R$ mediates anomalous angiogenesis with impaired integrity in tumors, with consequent increased metastases, is supported by the finding that administration of a specific $CysLT_2R$ antagonist, $BayCysLT_2$, recapitulated the protection with genetic deletion of $CysLT_2R$. In contrast, $CysLT_1R$ on colon epithelial cells promotes tumorigenesis, and high nuclear expression of $CysLT_1R$ is associated with a poor prognosis in patients with colorectal cancer (32, 33). This discrepancy may be the result of differences in the expression pattern of $CysLT_1R$ and $CysLT_2R$ in lung and colon tumor cells and related differences in tumor microenvironment.

Although our data reveal a prominent role for $CysLT_2R$ in ECs in regulating tumor angiogenesis and metastasis, we cannot rule out the contribution that $CysLT_2R$ has in other cell types. A mutant $CysLT_2R$ has been identified as a uveal melanoma oncogene, acting via $G\alpha_q$ signaling (13). LTs derived from neutrophils have been shown to play an important role in the colonization of distant tissues by a subpool of cancer cells retaining high tumor-initiating potential, with enhanced $CysLT_2R$ expression in human metastatic breast carcinoma and lymph node metastasis (34). Although we had similar overall leukocyte recruitment to the tumors in the presence or absence of CysLTRs, without the information on cell-specific immune cell recruitment to the tumor, our data cannot

rule out the contribution of $CysLT_2R$ on immune cells in regulating tumor cells and associated immune suppression. However, our data demonstrating (*i*) increased expression of $CysLT_2R$ in tumor vasculature in WT mice; (*ii*) disruption of the EC barrier and increased EC permeability by $CysLT_2R$-sufficient versus -deficient strains; and (*iii*) reduced tumor growth, angiogenesis, permeability, and metastasis, with a simultaneous increase in the pericyte coverage, in *Cysltr2*$^{-/-}$ and $BayCysLT_2$-treated mice unequivocally support that $CysLT_2R$ plays an important role in tumor growth and metastasis via its effect on ECs.

Materials and Methods

Mice. Male WT C57BL/6 (WT) mice (6–8 wk old) were purchased from The Jackson Laboratory. *Cysltr1*$^{-/-}$ and *Cysltr2*$^{-/-}$ mice on a C57BL/6 background were generated as described previously (35, 36). The mice were maintained at the Comparative Medicine Unit at Northeast Ohio Medical University (NEOMED) and the University of Akron (UA). All animal experiments were done in accordance with standard guidelines as approved by the Animal Care and Use Committees of NEOMED and the UA.

Matrigel Tube Formation Assay. MDECs and MLECs (8×10^4 cells) suspended in 0.5% serum-containing media were added to Growth Factor Reduced Matrigel (Corning) in the presence or absence of indicated agonists for 12–16 h. Cells were fixed, and images were taken on an EVOS XL Core phase-contrast microscope. Tubes were manually counted using ImageJ software (NIH), as described previously (17) and in *SI Appendix, SI Materials and Methods*.

Ex Vivo Mouse Aortic Ring Assay. An ex vivo mouse aortic ring assay was performed as described previously (37). Details are described in *SI Appendix, SI Materials and Methods*.

In Vivo Matrigel Plug Assay. Phenol-free Matrigel (Corning) containing 25 mg/mL heparin (Sigma–Aldrich) and 200 ng/mL bFGF with or without LTD_4 (500 nM) in a total volume of 500 μL was injected s.c. into both flanks of WT, *Cysltr1*$^{-/-}$, and *Cysltr2*$^{-/-}$ mice. Matrigel plugs were harvested 21 d after implantation, imaged, embedded in optimal cutting temperature compound, and stored at −80 °C until sectioning.

Gap Formation. An endothelial contraction assay was performed as described previously (15). Details are described in *SI Appendix, SI Materials and Methods*.

In Vitro Endothelial Permeability Assay. ECs from WT, *Cysltr1*$^{-/-}$, and *Cysltr2*$^{-/-}$ mice were cultured on a gelatin-coated, 1.0-μm pore size transwell (Corning) in a 24-well plate. Cells were treated with or without LTD_4 (500 nM) alone or with MK571 (1 μM) or $BayCysLT_2$ (1 μM) for 1 h and then incubated with 70 kDa of Texas Red-conjugated dextran for 1 h. One hundred microliters of each solution in plate wells was taken into a 96-well plate, and fluorescent signal corresponding leakiness was read using a Synergy H1 Microplate Reader (Biotek).

Syngeneic LLC Tumor Model and Metastasis. Tumors were implanted and analyzed as described previously (38). Details are described in *SI Appendix, SI Materials and Methods*.

ACKNOWLEDGMENTS. This study was supported by American Heart Association Grant 15GRNT25670004 and by a James Foght Assistant Professorship.

1. Ago H, et al. (2007) Crystal structure of a human membrane protein involved in cysteinyl leukotriene biosynthesis. *Nature* 448:609–612.
2. Colazzo F, Gelosa P, Tremoli E, Sironi L, Castiglioni L (2017) Role of the cysteinyl leukotrienes in the pathogenesis and progression of cardiovascular diseases. *Mediators Inflamm* 2017:2432958.
3. Nicosia S, Capra V, Rovati GE (2001) Leukotrienes as mediators of asthma. *Pulm Pharmacol Ther* 14:3–19.
4. Arroyo AG, Iruela-Arispe ML (2010) Extracellular matrix, inflammation, and the angiogenic response. *Cardiovasc Res* 86:226–235.
5. Sprague AH, Khalil RA (2009) Inflammatory cytokines in vascular dysfunction and vascular disease. *Biochem Pharmacol* 78:539–552.
6. Kondeti V, et al. (2013) Differential regulation of cysteinyl leukotriene receptor signaling by protein kinase C in human mast cells. *PLoS One* 8:e71536.
7. Maekawa A, Kanaoka Y, Xing W, Austen KF (2008) Functional recognition of a distinct receptor preferential for leukotriene E4 in mice lacking the cysteinyl leukotriene 1 and 2 receptors. *Proc Natl Acad Sci USA* 105:16695–16700.
8. Soter NA, Lewis RA, Corey EJ, Austen KF (1983) Local effects of synthetic leukotrienes (LTC4, LTD4, LTE4, and LTB4) in human skin. *J Invest Dermatol* 80:115–119.
9. Barrett NA, et al. (2012) Cysteinyl leukotriene 2 receptor on dendritic cells negatively regulates ligand-dependent allergic pulmonary inflammation. *J Immunol* 189:4556–4565.
10. Oyoshi MK, et al. (2012) Eosinophil-derived leukotriene C4 signals via type 2 cysteinyl leukotriene receptor to promote skin fibrosis in a mouse model of atopic dermatitis. *Proc Natl Acad Sci USA* 109:4992–4997.
11. Bankova LG, et al. (2016) Leukotriene E4 elicits respiratory epithelial cell mucin release through the G-protein-coupled receptor, GPR99. *Proc Natl Acad Sci USA* 113:6242–6247.
12. Bankova LG, et al. (2018) The cysteinyl leukotriene 3 receptor regulates expansion of IL-25-producing airway brush cells leading to type 2 inflammation. *Sci Immunol* 3:eaat9453.
13. Moore AR, et al. (2016) Recurrent activating mutations of G-protein-coupled receptor CYSLTR2 in uveal melanoma. *Nat Genet* 48:675–680.
14. Melero-Martin JM, et al. (2007) In vivo vasculogenic potential of human blood-derived endothelial progenitor cells. *Blood* 109:4761–4768.
15. Duah E, et al. (2013) Cysteinyl leukotrienes regulate endothelial cell inflammatory and proliferative signals through $CysLT_2$ and $CysLT_1$ receptors. *Sci Rep* 3:3274.
16. Komarova Y, Malik AB (2010) Regulation of endothelial permeability via paracellular and transcellular transport pathways. *Annu Rev Physiol* 72:463–493.
17. Adapala RK, et al. (2016) Activation of mechanosensitive ion channel TRPV4 normalizes tumor vasculature and improves cancer therapy. *Oncogene* 35:314–322.
18. Carmeliet P, Jain RK (2011) Principles and mechanisms of vessel normalization for cancer and other angiogenic diseases. *Nat Rev Drug Discov* 10:417–427.
19. Paruchuri S, et al. (2008) Leukotriene E4 activates peroxisome proliferator-activated receptor gamma and induces prostaglandin D2 generation by human mast cells. *J Biol Chem* 283:16477–16487.
20. Ni NC, et al. (2011) A selective cysteinyl leukotriene receptor 2 antagonist blocks myocardial ischemia/reperfusion injury and vascular permeability in mice. *J Pharmacol Exp Ther* 339:768–778.
21. Uzonyi B, et al. (2006) Cysteinyl leukotriene 2 receptor and protease-activated receptor 1 activate strongly correlated early genes in human endothelial cells. *Proc Natl Acad Sci USA* 103:6326–6331.
22. Barajas-Espinosa A, et al. (2012) The cysteinyl leukotriene 2 receptor mediates retinal edema and pathological neovascularization in a murine model of oxygen-induced retinopathy. *FASEB J* 26:1100–1109.
23. Moos MP, Funk CD (2008) Endothelial cysteinyl leukotriene 2 receptor expression and myocardial ischemia/reperfusion injury. *Trends Cardiovasc Med* 18:268–273.
24. Ridley AJ, Hall A (1992) The small GTP-binding protein rho regulates the assembly of focal adhesions and actin stress fibers in response to growth factors. *Cell* 70:389–399.
25. Haidari M, et al. (2011) Myosin light chain phosphorylation facilitates monocyte transendothelial migration by dissociating endothelial adherens junctions. *Cardiovasc Res* 92:456–465.
26. Kanayasu T, et al. (1989) Leukotriene C4 stimulates angiogenesis in bovine carotid artery endothelial cells in vitro. *Biochem Biophys Res Commun* 159:572–578.
27. Tsopanoglou NE, Pipili-Synetos E, Maragoudakis ME (1994) Leukotrienes C4 and D4 promote angiogenesis via a receptor-mediated interaction. *Eur J Pharmacol* 258:151–154.
28. Xu L, et al. (2010) Involvement of cysteinyl leukotriene receptors in angiogenesis in rat thoracic aortic rings. *Pharmazie* 65:750–754.
29. Reynolds AL, et al. (2016) Phenotype-based discovery of 2-[(E)-2-(Quinolin-2-yl)vinyl]phenol as a novel regulator of ocular angiogenesis. *J Biol Chem* 291:7242–7255.
30. Abramsson A, Lindblom P, Betsholtz C (2003) Endothelial and nonendothelial sources of PDGF-B regulate pericyte recruitment and influence vascular pattern formation in tumors. *J Clin Invest* 112:1142–1151.
31. Compagni A, Wilgenbus P, Impagnatiello MA, Cotten M, Christofori G (2000) Fibroblast growth factors are required for efficient tumor angiogenesis. *Cancer Res* 60:7163–7169.
32. Magnusson C, et al. (2010) Low expression of CysLT1R and high expression of CysLT2R mediate good prognosis in colorectal cancer. *Eur J Cancer* 46:826–835.
33. Savari S, et al. (2016) Cysteinyl leukotriene 1 receptor influences intestinal polyp incidence in a gender-specific manner in the ApcMin/+ mouse model. *Carcinogenesis* 37:491–499.
34. Wculek SK, Malanchi I (2015) Neutrophils support lung colonization of metastasis-initiating breast cancer cells. *Nature* 528:413–417.
35. Beller TC, Maekawa A, Friend DS, Austen KF, Kanaoka Y (2004) Targeted gene disruption reveals the role of the cysteinyl leukotriene 2 receptor in increased vascular permeability and in bleomycin-induced pulmonary fibrosis in mice. *J Biol Chem* 279:46129–46134.
36. Maekawa A, Austen KF, Kanaoka Y (2002) Targeted gene disruption reveals the role of cysteinyl leukotriene 1 receptor in the enhanced vascular permeability of mice undergoing acute inflammatory responses. *J Biol Chem* 277:20820–20824.
37. Bellacen K, Lewis EC (2009) Aortic ring assay. *J Vis Exp,* e1564.
38. Thoppil RJ, et al. (2015) TRPV4 channel activation selectively inhibits tumor endothelial cell proliferation. *Sci Rep* 5:14257.